

Article

Temperature-Dependent Creep Behavior and Quasi-Static Mechanical Properties of Heat-Treated Wood

Dong Xing ^{1,*}, Xinzhou Wang ²  and Siqun Wang ³ ¹ College of Materials Science and Art Design, Inner Mongolia Agriculture University, Hohhot 010018, China² College of Materials Science and Engineering, Nanjing Forestry University, Nanjing 210037, China; xzwwang@njfu.edu.cn³ Center for Renewable Carbon, University of Tennessee, Knoxville, TN 37996, USA; swang@utk.edu

* Correspondence: xingdong@imau.edu.cn

Abstract: In this paper, Berkovich depth-sensing indentation has been used to study the effects of the temperature-dependent quasi-static mechanical properties and creep deformation of heat-treated wood at temperatures from 20 °C to 180 °C. The characteristics of the load–depth curve, creep strain rate, creep compliance, and creep stress exponent of heat-treated wood are evaluated. The results showed that high temperature heat treatment improved the hardness of wood cell walls and reduced the creep rate of wood cell walls. This is mainly due to the improvement of the crystallinity of the cellulose, and the recondensation and crosslinking reaction of the lignocellulose structure. The Burgers model is well fitted to study the creep behavior of heat-treated wood cell walls under different temperatures.

Keywords: heat-treated wood; nanoindentation; temperature-dependent; creep behavior



Citation: Xing, D.; Wang, X.; Wang, S. Temperature-Dependent Creep Behavior and Quasi-Static Mechanical Properties of Heat-Treated Wood. *Forests* **2021**, *12*, 968. <https://doi.org/10.3390/f12080968>

Academic Editors: Joseph E. Jakes and Angela Lo Monaco

Received: 21 June 2021
Accepted: 19 July 2021
Published: 22 July 2021

Publisher's Note: MDPI stays neutral with regard to jurisdictional claims in published maps and institutional affiliations.



Copyright: © 2021 by the authors. Licensee MDPI, Basel, Switzerland. This article is an open access article distributed under the terms and conditions of the Creative Commons Attribution (CC BY) license (<https://creativecommons.org/licenses/by/4.0/>).

1. Introduction

As a kind of complex natural polymer material, wood exhibits obvious viscoelastic properties, such as creep and stress relaxation [1–3]. The viscoelasticity of wood is very sensitive to changes in service temperature, moisture content and wood species [4–6]. Wood heat treatment can effectively improve the defects of cracking, warping deformation and easy decay of wood material [7,8]. Therefore, heat-treated wood with elegant color and dimensional stability is widely used for furniture, flooring, cladding and outdoor utilities [9], while the mechanical properties of the heat-treated wood are critical for its modification and application [10]. Most previous studies were focused on the changes of micromechanical properties of cell walls with different heat treatments that use nanoindentation [11,12]. Nanoindentation is widely used to characterize the quasi-static mechanical properties of metals and polymers at the micro scale [13–15]. The quasi-static mechanical properties of samples are measured by the stress–strain curves under constant load [15]. Nanoindentation is also applicable to the study of plastic deformation and dislocations of materials [16–18]. The creep of materials such as polymers and soft metals has been studied using data collected during the pressing process [19,20]. Nanoindentation is also applied to characterize the viscoelastic properties of biological tissue structure by extending the load-holding time [21]. In previous studies, the creep model has provided an interesting explanation for the rheological behavior of chemical-modified materials [22–24]. Creep is an important form of viscoelastic behavior of wood, which includes stress relaxation and dynamic viscoelasticity [25]. As a complex organic polymer, wood exhibits viscoelastic behavior due to the movement of molecular chain segments, flow within molecules, slip between molecules, crystallization and molecular orientation [26,27].

There is no published study on the micro-mechanical creep deformation of heat-treated wood under different service temperatures. This study of the viscoelasticity of heat-treated wood provides the fundamental theoretical basis for heat treatment. The

purpose of this paper is to test the hypothesis that heat treatment can reduce the creep ratio of wood at high temperatures and to provide a theoretical basis for the use of heat-treated wood as wood flooring. The temperature-dependent creep characteristics of heat-treated wood subjected to sustained constant stress were measured.

2. Materials and Methods

2.1. Materials

Larch (*Larix gmelinii* (Rupr.) Kuzen) is a rapid planting species in artificial forests, which is widely distributed in Northern and eastern China due to its excellent adaptability. The dimensions of the sample are 10 mm, 8 mm and 8 mm (axial, radial and tangential), respectively. The bottom and top of the samples are parallel and perpendicular to the axial section of wood cell wall. Samples were precisely prepared from the same growth ring and the late wood location of the growth ring was marked. The samples were placed in an oven for 48 h conventional drying at 103 °C. All samples were then placed in moisture-proof plastic bags for high temperature heat treatment.

2.2. Heat Treatment

After a conventional drying process, the wood specimens were treated by 1'' tube furnace (Thermo Scientific, Asheville, NC, USA) at 180 ± 1 °C and 210 ± 1 °C for 6 h. Nitrogen was used as the shielding and heat conduction gas for heat treatment and the gas flow rate was 20 mL/min. All specimens were then deposited in an oven at 103 °C to await nanoindentation testing. The specific parameters of the heat treatment process were consistent with previous studies [28]. H0 refers to the oven-dry sample, and H1 and H2 are the heat-treated samples at 180 °C and 210 °C.

Quasi-static nanoindentation:

The wood samples were fixed onto a sample holder. The samples were well prepared into a pyramid shape. Then, the tips of samples were smoothed using an ultramicrotome equipped with glass and diamond knives. Preparation of the samples followed the steps represented by Meng [5].

A TriboIndenter (Hysitron Inc., Minneapolis, MN, USA), integrated with a Berkovich diamond tip and operated in open-loop control mode, was applied to measure the wood S2 layer cell wall laminae.

On the basis of nanoindentation, the micro-mechanical properties (hardness and elastic modulus) were obtained from the load–displacement curves:

Hardness:

$$H = \frac{P_{max}}{A} \quad (1)$$

P_{max} is the peak load force and A is acquired by the projected contact area.

The sample's reduced elastic modulus (E_r) was obtained as follows:

$$E_r = \frac{dP}{dh} \times \frac{1}{2} \times \frac{\sqrt{\pi}}{\sqrt{A}} \quad (2)$$

where dP/dh (stiffness) is the slope of the line of the unloading process.

The thermal stage is used to achieve a temperature control stage for different service temperatures by means of the nanoindentation test. The three-segment load ramp of the indentation experiment was performed, including: load time for 5 s, load-holding process for 30 s and unloading process for 5 s, as seen in Figure 1. The peak load force of nanoindentation was 400 μN for all tests. An indentation depth of 150~200 nm was achieved on the wood cell wall, as seen in Figure 2. Figure 2a shows the morphology of the cell wall under scanning electron microscope, and Figure 2b–d show the SPM scanning images before and after indentation to verify the validity of the indentation data. The samples were indentation tested at 20 °C, 60 °C, 100 °C, 140 °C and 180 °C for wood specimens. The nanoindentations were performed under ambient relative humidity, which was $45 \pm 2\%$ during the experimental procedure.

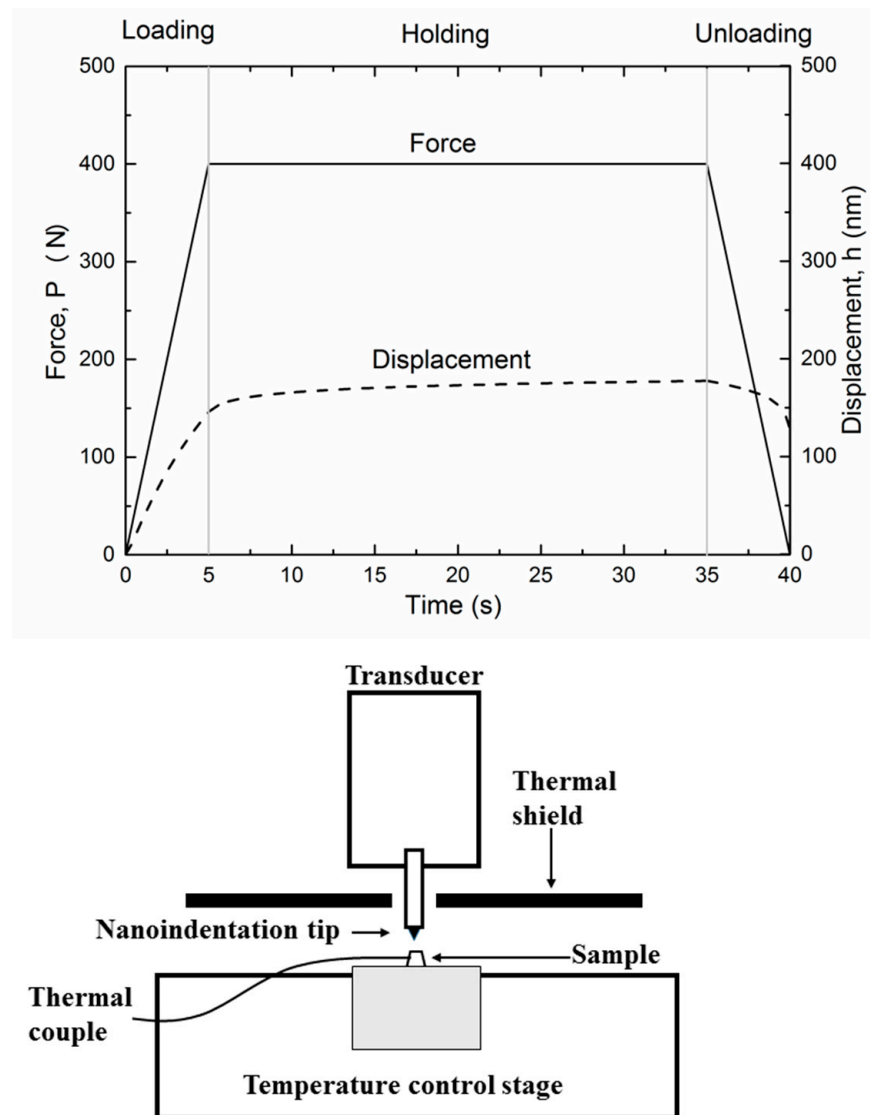


Figure 1. The load force–displacement curve of nanoindentation and the schematic diagram of the nanoindentation system [28].

2.3. Viscoelastic Properties-Creep Behavior Nanoindentation Test

The short-term viscoelastic behavior of heat-treated wood cell walls was investigated under constant load. Nanoindentation equipped with a Berkovich tip was used to study the effect of the temperature-dependent hardness, modulus and short-term mechanical creep behavior from room temperature to 180 °C. For nanoindentation, the creep strain rate was obtained through the following equations. The stress can be calculated as follows.

$$\frac{d\varepsilon}{dt} = \frac{1}{h} \frac{dh}{dt} \quad (3)$$

$$\sigma = \frac{P}{A} = \frac{P}{24.5h^2} \quad (4)$$

where $d\varepsilon/dt$ is the creep strain rate, h is the indent depth, t is the creep time, σ is the stress, P is the constant peak loading force and A is the indent contact area. A is the projected contact area given in our present work.

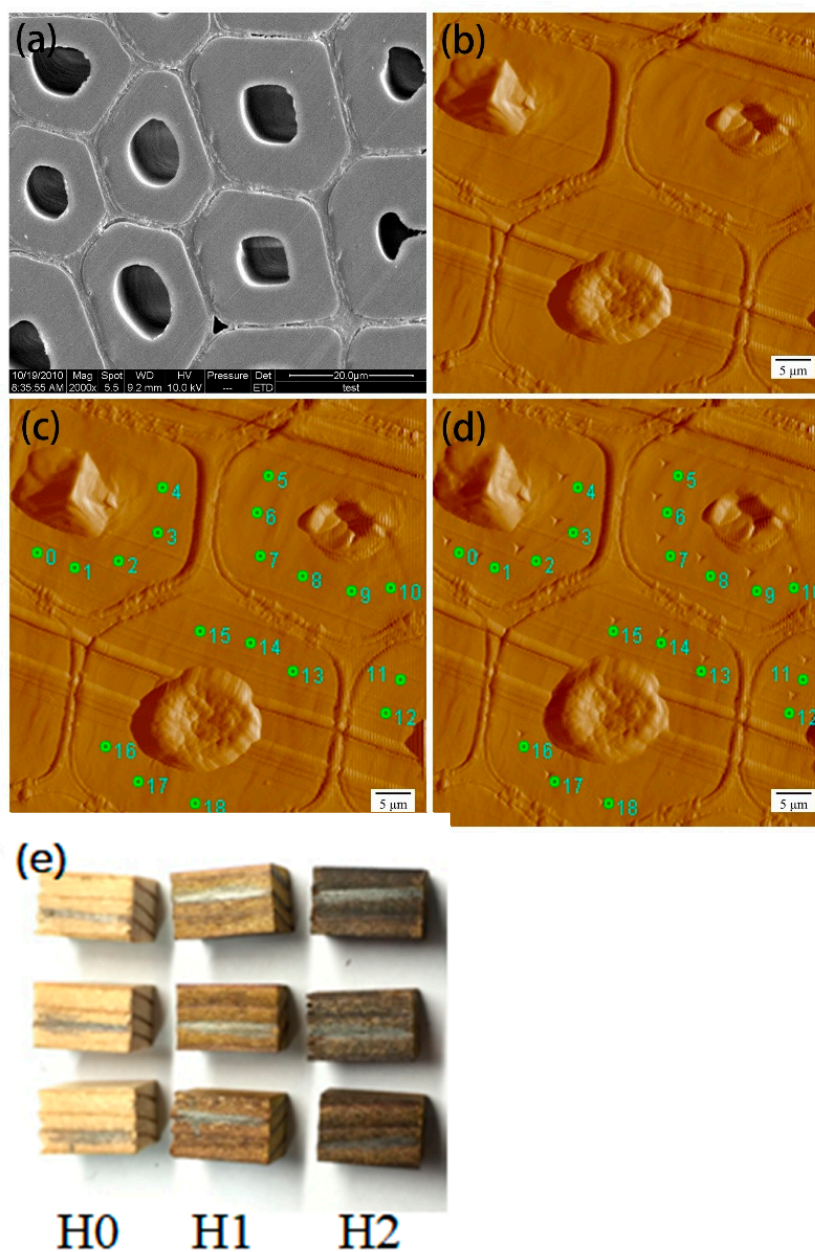


Figure 2. The image of SEM/SPM image before and after nanoindentation and the samples before and after heat treatment: (a) SEM image; (b) wood cell wall before indentation; (c) the marks of indentation; (d) after indentation; (e) wood samples before and after heat treatment.

Based on the curves of indent depth versus time, the creep strain rate can be obtained. The creep strain rates of samples are strongly dependent on the stress. The creep data of wood cell wall can be obtained by nanoindentation test. The strain and creep compliance of wood cell wall can be calculated as follows.

$$\varepsilon(t) = \sigma_0 J(t) \quad (5)$$

Since

$$\varepsilon(t) = \frac{h(t)}{h_{in}} \quad (6)$$

and

$$\sigma_0 = \frac{P_0}{A_0} \quad (7)$$

Then, Equation (3) can be rewritten as

$$J(t) = \frac{A_0}{P_0 h_{in}} h(t) \quad (8)$$

Before nanoindentations, the wood samples were held at the testing temperature for 10 min to attain thermal equilibrium. The thermal stage was also added to measure the creep behavior of samples in different temperature conditions (ambient condition, 60 °C, 100 °C, 140 °C and 180 °C). At least 10 measurements were repeated and the average value, that could reduce the noise of the creep curves, was calculated.

Burgers model

The *Burgers* model was selected to simulate the experimental data and to investigate the heat-treated and untreated wood at different temperatures, respectively. The schematic image of the *Burgers* model is represented in Figure 3.

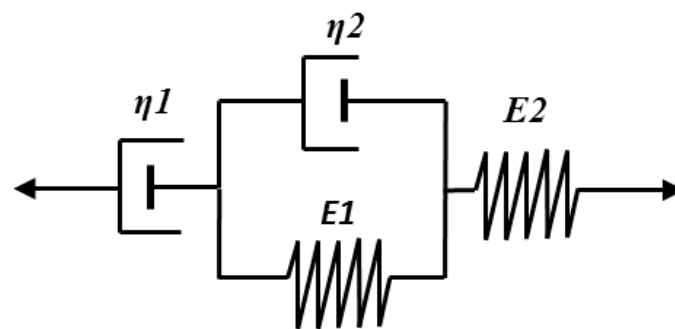


Figure 3. Schematic image of the Burgers model.

By applying the *Burgers* model, the creep compliance can be rewritten as follows:

$$J(t) = J_0 + J_1 t + J_2 \left[1 - \exp\left(-\frac{t}{\tau_0^B}\right) \right] \quad (9)$$

where $J_0 = 1/E_e^B$, $J_1 = 1/\eta_1^B$, $J_2 = 1/E_d^B$ and $\tau_0^B = \eta_2^B/E_d^B$. E_e^B and E_d^B are the spring constants, while η_1^B and η_2^B are the viscosity parameters of pure viscous damper shown in Figure 3.

3. Results and Discussion

3.1. Thermal Drift

The temperature of the hot stage was monitored by a thermocouple placed on the sample surface to detect the real time surface temperature. Figure 4 shows the thermal drift rate during the nanoindentation test. The thermal drift rate of each sample gradually increases with the increase in the test temperature. After proper temperature balance is attained, all the drift rates are controlled and kept at less than 1.2 nm/s. Therefore, the thermal drift has little effect on the test results [29].

3.2. Temperature on Quasi-Static Mechanical Properties

Figure 5a,b show the reduced elastic modulus and hardness of the wood cell wall of heat-treated and untreated wood at different temperatures, where the error line represents the standard deviation of the samples. The elastic modulus and hardness of untreated samples increased with the increase in ambient temperature from 20 °C to 100 °C. The increasing trend is mainly caused by the reduction in the moisture content of the samples during the temperature increase [28]. The reduction in moisture content of wood caused the decrease in the mobility of cellulose molecular chains and chain segments, which contributes to the increase in elastic modulus and hardness [18]. The moisture content of the heat-treated wood is lower than that of the untreated wood, so the hardness and elastic

modulus of the heat-treated wood are less affected by the ambient temperature (20 °C to 100 °C). The hardness and elastic modulus of H0 decreased noticeably with the service temperature being raised above 140 °C, which included the softening process of wood and the mild pyrolysis of wood components (especially the hemicellulose degradation) [7]. The gas environment of the sample in the nanoindentation test process caused the oxidation reaction of the extract and the pyrolysis of the wood's main components [8]. Large deviation values of H0 hardness and elastic modulus at 140 °C and 180 °C also indicate that wood cell walls undergo complex chemical reactions at this time. In other words, the nanoindentation test at 180 °C can also be viewed as an air heat treatment, while the hardness and elastic modulus of H1 and H2 samples showed small fluctuations, indicating that the high temperature (140 °C~180 °C) environment has less effect on the heat-treated samples. The heat-treated wood has better high temperature resistance, which is caused by the decrease in the hemicellulose content, cellulose recondensation and cross-linking reactions of the lignin structure [5].

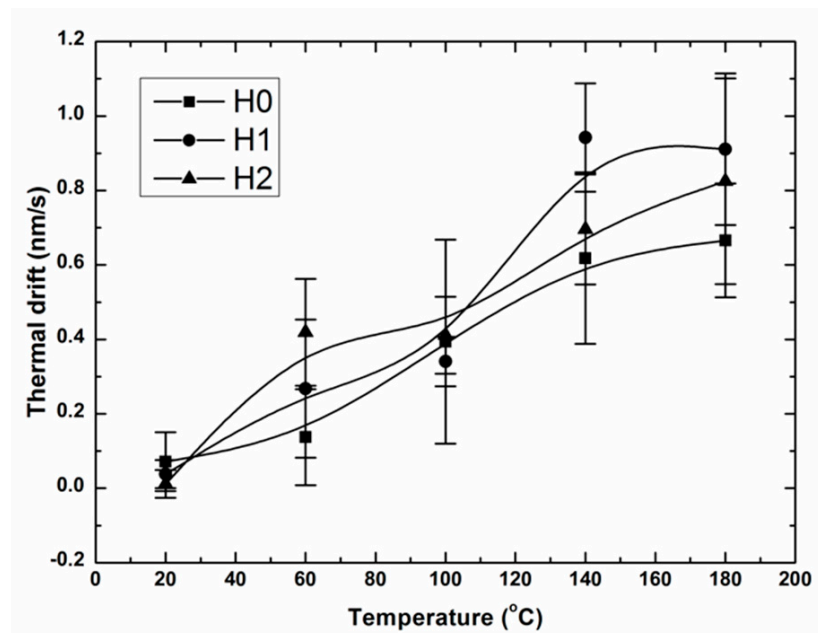


Figure 4. Thermal drift rate with different service temperatures.

3.3. Temperature on Creep Behaviors

Generally, wood creep occurs under compressive stress, which is related to the variation of wood species, mechanical properties, stress level, temperature, moisture content and other factors [1,4,28]. The parameters of the creep behavior of the cell walls were obtained from the data recorded in the nanoindentation peak force-holding process. The displacement–time curve of untreated wood at different service temperatures is shown in Figure 6. The displacement increased rapidly at the beginning of loading and then slowed down gradually. This creep behavior consists of instantaneous elastic deformation, viscoelastic deformation and viscoelastic degeneration [19,20]. The maximum creep displacement of H0 occurs at 20 °C. For the H0 nanoindentation test at 180 °C, the creep displacement increased significantly, and the curve fluctuated noticeably; this is mainly caused by the degradation of hemicellulose and the softening of lignin [16]. For the high temperature nanoindentation test, the movement of the cellulose molecular chain was activated, the free volume gradually increased, and the intermolecular chain began to slip [30]. Hydrogen bonds between hemicellulose and cellulose in the amorphous region were broken, which also promoted the creep displacement [16,28].

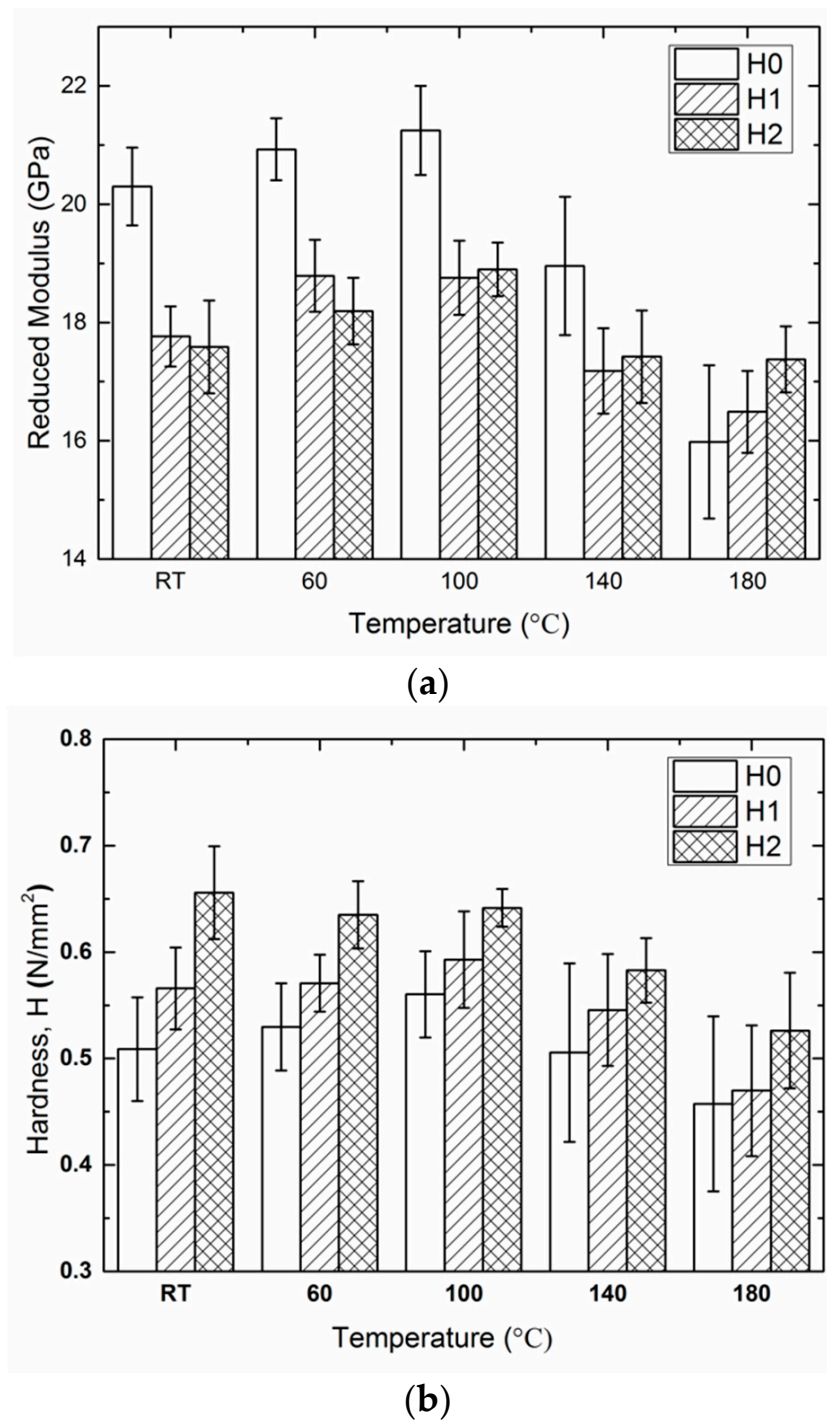


Figure 5. (a) The reduced modulus of heat-treated and untreated wood cell wall; (b) the hardness of heat-treated and untreated wood cell wall.

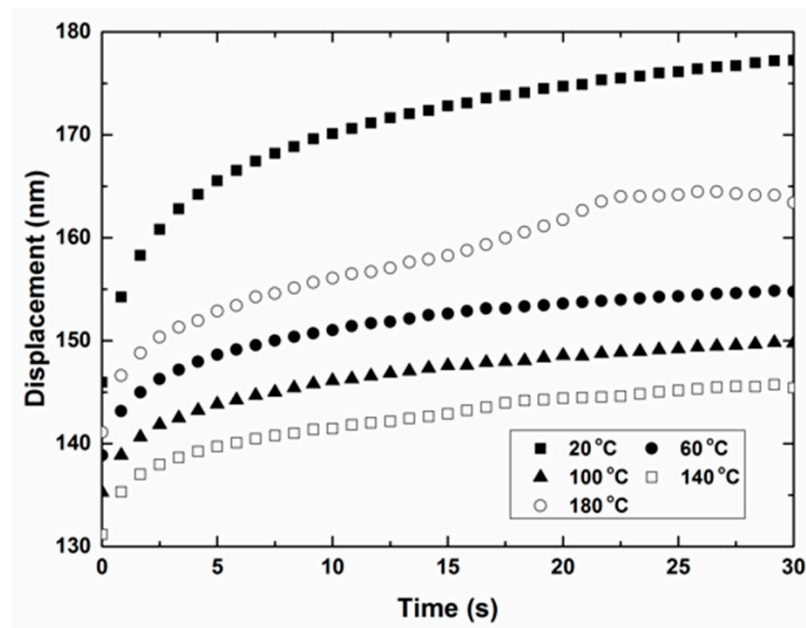


Figure 6. The creep displacement of untreated wood cell wall.

3.4. Heat Treatment on Creep Behaviors

According to the microstructure of wood, the cell wall can be seen as complex ligno-cellulosic composites [13]. The nanoindentation is mainly applied to the S2 layer of the cell wall, which is the thickest part of the cell wall [1,5]. Figure 7 shows the creep compliance for different test temperature conditions (20 °C, 60 °C, 100 °C, 140 °C and 180 °C) of H0, H1 and H2. Comparing the H0, H1 and H2 curves at the same test temperature, it is clear that the heat treatment completely changes the wood cell wall creep behavior. In Figure 7, the creep compliance of the cell wall is decreased after heat treatment at room temperature (20 °C). In other words, heat treatment can effectively reduce the creep behavior of the wood cell walls at 20 °C. H2 exhibits minimal creep compliance from room temperature to 100 °C, while it represents the maximum creep compliance at 180 °C. The creep of H2 sample increases rapidly when ambient temperature exceeds 100 °C. In addition, the H0 and H1 curves overlap when the ambient temperature reaches 140 °C, which is most likely caused by hemicellulose Softening. As a complex physical modification process, heat treatment includes the degradation and modification of hemicellulose [30], the degradation and crystallization of amorphous cellulose and the condensation polymerization of lignin [31,32]. After heat treatment, the reinforced wood cell walls showed less creep, which was closely correlated with the tighter bond of the wood cell wall.

3.5. Burgers Model

Nanoindentation is widely applied in the microscopic creep deformation of materials [33,34]. This study shows that nanoindentation technology can effectively test the heat treatment of wood cell wall creep behavior. The experimental data are simulated using the four component Burgers model. Figures 8 and 9 show the experimental data for wood cell wall creep compliance and the red line is creep compliance simulated by the Burgers model. The creep simulated curves are in good agreement with the test data, with a goodness of fit of 0.99. The Burgers model is suitable for forecasting the creep behavior of wood cell walls. According to nanoindentation test data, the creep parameters of wood cell walls are obtained based on Burgers model fitting. The parameters of the Burgers model include $E1$, $E2$, $\eta1$, $\eta2$ and $\tau0$: elastic modulus, viscoelastic modulus, plasticity coefficient, viscoelasticity and relaxation time. These parameters are listed in Table 1.

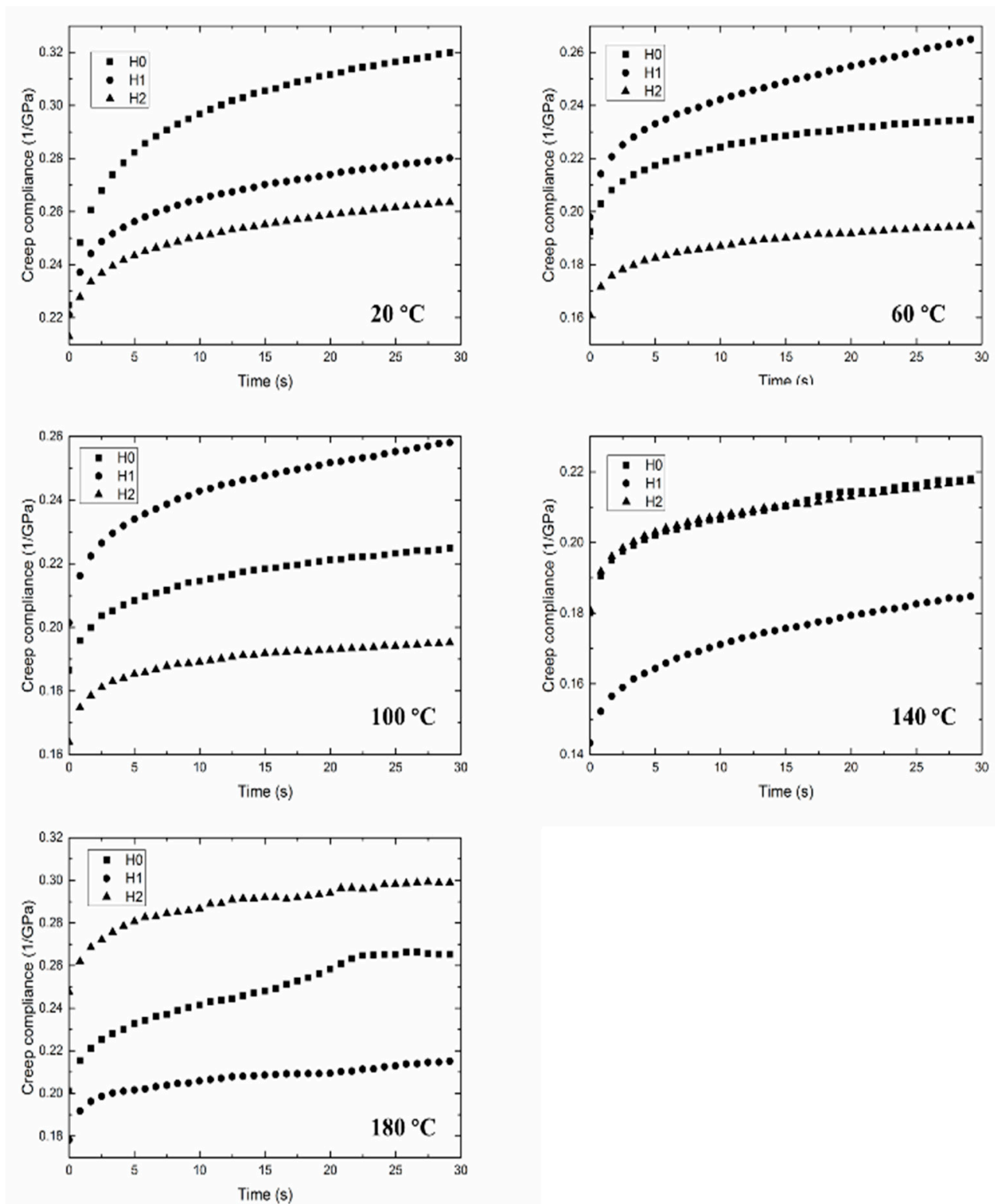


Figure 7. The effect of heat treatment on the creep compliance of the wood cell wall.

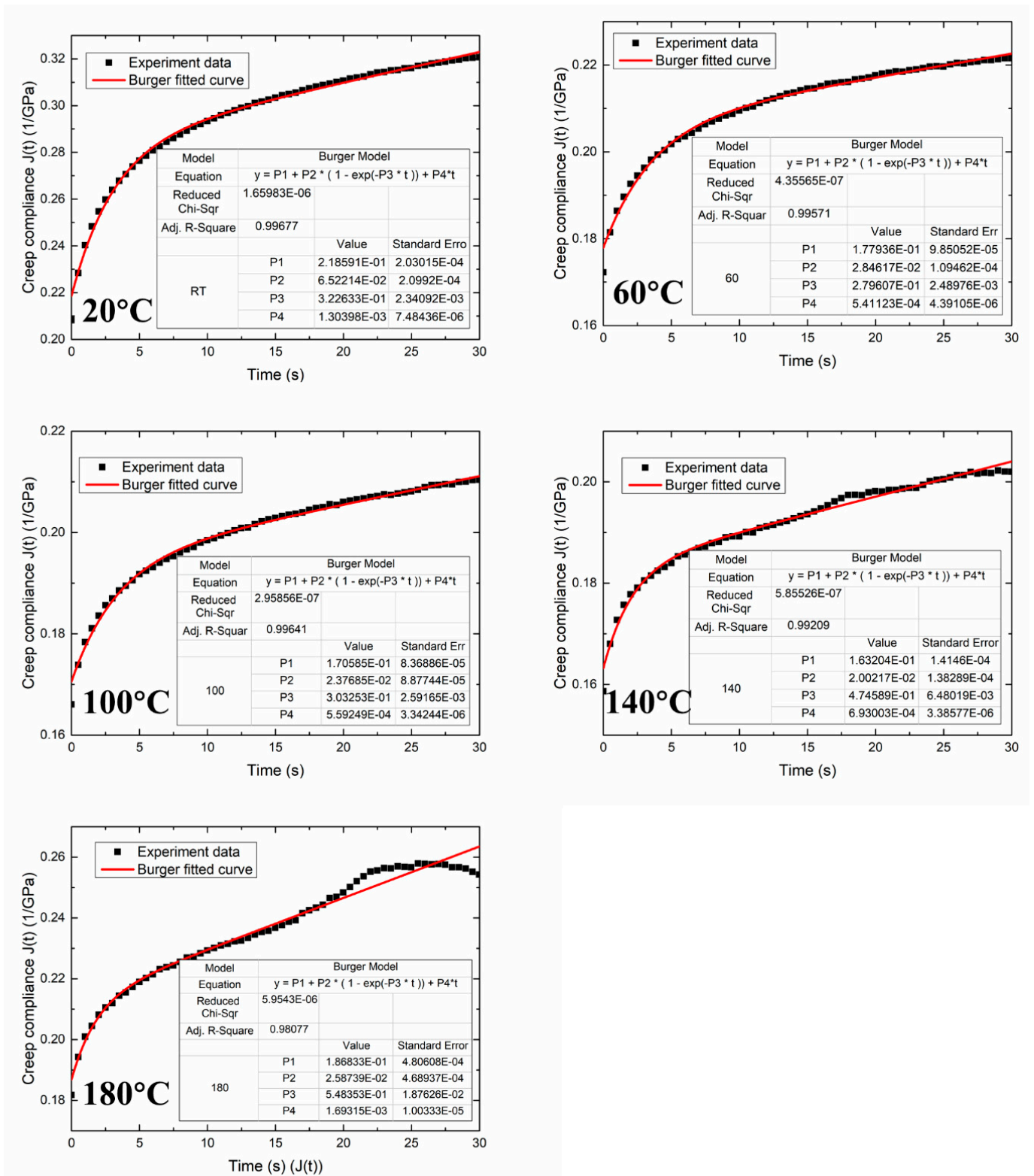


Figure 8. The test data and simulated curves of untreated wood cell wall.

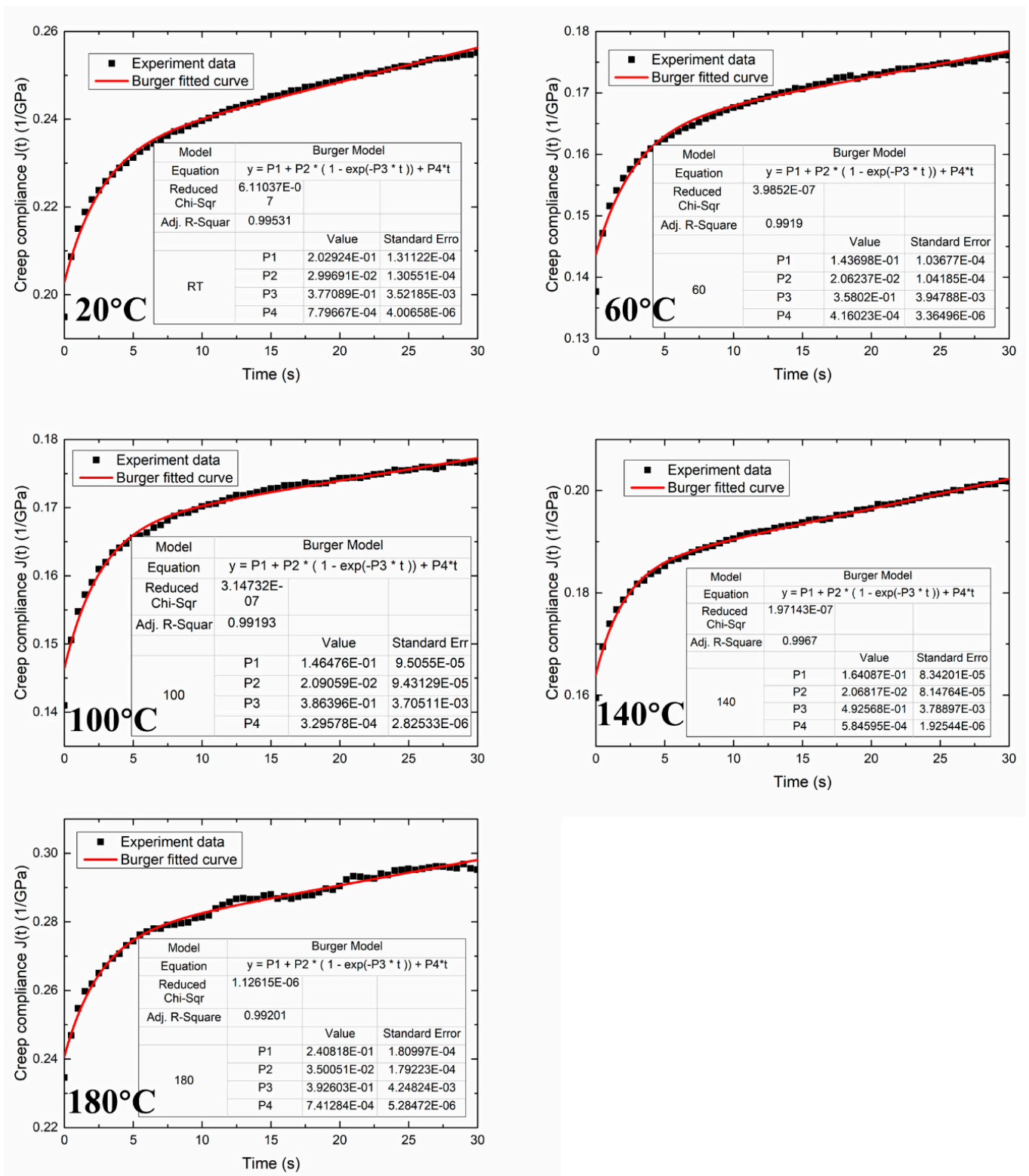


Figure 9. The test data and simulated curves of H2 heat-treated wood cell wall.

Table 1. Parameters of Burgers model.

Temp (°C)	No.	E ₁ (GPa)	E ₂ (GPa)	η ₁ (GPa·S)	η ₂ (GPa·S)	τ ₀ (S)	R ²
20	H0	4.57	15.33	769.23	47.52	3.10	0.997
	H1	4.71	27.99	1086.19	74.20	2.65	0.996
	H2	4.93	33.37	1282.60	88.48	2.65	0.995
60	H0	5.62	35.14	1848.01	125.66	3.58	0.996
	H1	5.42	31.40	719.42	67.52	2.15	0.998
	H2	6.96	48.50	2403.71	135.46	2.79	0.992
100	H0	5.86	42.07	1788.11	138.73	3.30	0.996
	H1	5.29	29.88	1097.24	81.92	2.74	0.997
	H2	6.83	47.82	3034.18	123.77	2.59	0.992
140	H0	6.13	49.95	1443.00	105.25	2.11	0.992
	H1	8.13	49.02	1315.31	155.38	3.17	0.998
	H2	6.09	48.36	1710.59	98.17	2.03	0.997
180	H0	5.35	38.65	591.72	70.49	1.82	0.981
	H1	6.25	44.70	1736.70	55.56	1.24	0.990
	H2	4.15	28.56	1349.01	72.75	2.55	0.992

The creep deformation of wood is greatly affected by heat treatment, environmental temperature and humidity [5,35]. At room temperature, the Burgers models E_1 , E_2 , η_1 and η_2 of the wood cell walls increased gradually with the increase in heat treatment intensity, as seen in Table 1. This demonstrates that heat treatment can reduce wood cell wall creep behavior at room temperature, which is consistent with results obtained using the quasi-static nanoindentation test [18,28]. When the service temperature increased (60~140 °C), the elastic modulus, viscoelastic modulus, plastic coefficient and viscoelasticity of the untreated specimen showed a significant increase, which is related to the softening of the wood cell wall. The creep parameters of the Burgers model of the untreated sample were significantly reduced and there was a significant fluctuation in the creep curve at 180 °C, which was caused by real-time softening and pyrolysis of the wood components during the 180 °C nanoindentation test. Compared with the untreated sample, the creep curve of H2 is relatively stable at 180 °C. The results showed that the Burgers model was well fitted to the creep curves of untreated and heat-treated Larix cell wall. The difference between the fitting data of the Burgers model and the experimental data is accurately controlled.

4. Conclusions

After reasonable temperature balance treatment, the nanoindentation overcomes the limitations of the inherent room temperature test and can be used to test the microscopic creep behavior under high temperature conditions. The hardness of the wood cell walls significantly increased and the creep rate decreased noticeably after heat treatment. The improvement in the micromechanical properties of wood after heat treatment is mainly due to the recondensation and cross-linking reaction of the lignocellulosic structure and the increase in the crystallinity of cellulose.

It has been verified that the parameters of creep behavior fitted by the Burgers model are sensitive to changes in ambient temperature. The Burgers model can adequately fit the creep of wood cell walls under temperature response.

The nanoindentation test during the peak stress holding stage also demonstrated the softening of wood components at high temperature. It was also proven that the Burgers model is appropriate to study the viscoelastic creep behavior of wood cell walls.

Author Contributions: Conceptualization, D.X., X.W. and S.W.; methodology, D.X.; software, D.X.; validation, D.X. and S.W.; formal analysis, D.X., X.W. and X.W.; investigation, D.X.; resources, D.X.; data curation, D.X. and S.W.; writing—original draft preparation, D.X.; writing—review and editing, D.X., X.W. and S.W.; visualization, D.X.; supervision, S.W.; project administration, D.X.; funding acquisition, D.X. All authors have read and agreed to the published version of the manuscript.

Funding: This research was funded by the National Natural Science Foundation of China (Grant No. 31700484) and the Research Start-Up Project of Inner Mongolia Agricultural University (NDYB 2017-4).

Conflicts of Interest: The authors declare no conflict of interest.

References

1. Wang, D.; Lin, L.; Fu, F. The difference of creep compliance for wood cell wall CML and secondary S2 layer by nanoindentation. *Mech. Time-Depend. Mater.* **2019**, *9*, 1–12. [[CrossRef](#)]
2. Passard, J.; Perré, P. Viscoelastic behaviour of green wood across the grain. Part II. A temperature dependent constitutive model defined by inverse method. *Ann. For. Sci.* **2005**, *62*, 823–830. [[CrossRef](#)]
3. Zhang, T.; Bai, S.L.; Zhang, Y.F.; Thibaut, B. Viscoelastic properties of wood materials characterized by nanoindentation experiments. *Wood Sci. Technol.* **2012**, *46*, 1003–1016. [[CrossRef](#)]
4. Bäder, M.; Németh, R.; Konnerth, J. Micromechanical properties of longitudinally compressed wood. *Eur. J. Wood Wood Prod.* **2019**, *77*, 341–351. [[CrossRef](#)]
5. Meng, Y.; Xia, Y.; Young, T.M.; Cai, Z.; Wang, S. Viscoelasticity of wood cell walls with different moisture content as measured by nanoindentation. *RSC Adv.* **2015**, *5*, 47538–47547. [[CrossRef](#)]
6. Kaufman, J.D.; Miller, G.J.; Morgan, E.F.; Klapperich, C.M. Time-dependent mechanical characterization of poly(2-hydroxyethyl methacrylate) hydrogels using nanoindentation and unconfined compression. *J. Mater. Res.* **2008**, *23*, 1472–1481. [[CrossRef](#)]
7. Esteves, B.; Cruz-Lopes, L.S.; Figueirinha, A.; Lemons, L.T.; Ferreira, J.; Pereira, H.; Domingos, I. Heat-treated wood as chromium adsorption material. *Eur. J. Wood Wood Prod.* **2017**, *75*, 903–909. [[CrossRef](#)]
8. Kufre, E.O.; Fengcai, L.; Yandan, C.; Biao, H. Effect of silicone oil heat treatment on the chemical composition, cellulose crystalline structure and contact angle of Chinese parasol wood. *Carbohydr. Polym.* **2017**, *164*, 179–185.
9. Nguyen, T.T.; Nguyen, T.H.V.; Ji, X.D.; Yuan, B.N.; Trinh, H.M.; Do, K.T.L.; Guo, M.H. Prediction of the color change of heat-treated wood during artificial weathering by artificial neural network. *Eur. J. Wood Wood Prod.* **2019**, *77*, 1107–1116. [[CrossRef](#)]
10. Chang, C.W.; Kuo, W.L.; Lu, K.T. On the Effect of Heat Treatments on the Adhesion, Finishing and Decay Resistance of Japanese cedar (*Cryptomeria japonica* D. Don) and Formosa acacia (*Acacia confuse* Merr. (Leguminosae)). *Forests* **2019**, *10*, 586. [[CrossRef](#)]
11. Yuan, H.; Tang, S.; Luo, Q.; Xiao, T.; Wu, Y. Micro-FTIR spectroscopy and partial least-squares regression for rapid determination of moisture content of nanogram-scaled heat-treated wood. *J. Wood Sci.* **2020**, *66*, 1–7. [[CrossRef](#)]
12. Delucis, R.; Beltrame, R.; Gatto, D.A. Discolouration of heat-treated fast-growing eucalyptus wood exposed to natural weathering. *Cell Chem. Technol.* **2019**, *53*, 635–641. [[CrossRef](#)]
13. Rindler, A.; Hansmann, C.; Konnerth, J. The effect of moisture on the mechanical response of wood, adhesive and their interphase by means of nanoindentation. *Wood Sci. Technol.* **2019**, *53*, 729–746. [[CrossRef](#)]
14. Liang, R.; Zhu, Y.H.; Yang, X.; Gao, J.S.; Cai, L.P. Study on the ultrastructure and properties of gelatinous layer in poplar. *J. Mater. Sci.* **2021**, *56*, 415–427. [[CrossRef](#)]
15. Lucca, D.A.; Herrmann, K.; Klopstein, M.J. Nanoindentation: Measuring methods and applications. *CIRP Ann.* **2010**, *59*, 803–819. [[CrossRef](#)]
16. Li, Y.; Huang, C.; Wang, L.; Wang, S.; Wang, X. The effects of thermal treatment on the nanomechanical behavior of bamboo (*Phyllostachys pubescens* Mazel ex H. De Lehaie) cell walls observed by nanoindentation, XRD, and wet chemistry. *Holzforschung* **2016**, *71*, 129–135. [[CrossRef](#)]
17. Xing, D.; Li, J.; Wang, S. Comparison of the chemical and micromechanical properties of *Larix* spp. after eco-friendly heat treatments measured by in situ nanoindentation. *Sci. Rep.* **2020**, *10*, 4358. [[CrossRef](#)] [[PubMed](#)]
18. Wang, X.; Zhao, L.; Deng, Y.; Li, Y.; Wang, S. Effect of the penetration of isocyanates (pMDI) on the nanomechanics of wood cell wall evaluated by AFM-IR and nanoindentation (NI). *Holzforschung* **2017**, *72*, 301–309. [[CrossRef](#)]
19. Chen, Y.P.; Guo, J.P.; Cai, Y.Y. An anisotropic distribution dislocation loop model for simulation of nanoindentation of single crystals. *Mech. Mater.* **2017**, *108*, 1–10. [[CrossRef](#)]
20. Han, R.; Wang, X.; Zhu, G.; Han, N.; Xing, F. Investigation on viscoelastic properties of urea-formaldehyde microcapsules by using nanoindentation. *Polym. Test.* **2019**, *80*, 106146. [[CrossRef](#)]
21. Shepherd, T.N.; Zhang, J.; Ovaert, T.C.; Roeder, R.K.; Niebur, G.L. Direct comparison of nanoindentation and macroscopic measurements of bone viscoelasticity. *J. Mech. Behav. Biomed.* **2011**, *4*, 2055–2062. [[CrossRef](#)] [[PubMed](#)]
22. Hadjab, I.; Farlay, D.; Crozier, P.; Douillard, T.; Follet, H. Intrinsic Properties of Osteomalacia Bone evaluated by Nanoindentation and FTIRM Analysis. *J. Biomech.* **2021**, *117*, 110247. [[CrossRef](#)] [[PubMed](#)]
23. Zhang, Z.N.; Tian, Z.Q.; Yuan, Z.Q.; Li, J.J.; Wu, W.P.; Xia, R. Temperature and loading sensitivity investigation of nanoindentation short-term creep behavior in Nafion (R). *Mater. Res. Express* **2019**, *6*, 055304. [[CrossRef](#)]
24. Liu, K.; Ostadhassan, M.; Bubach, B. Application of nanoindentation to characterize creep behavior of oil shales. *J. Pet. Sci. Eng.* **2018**, *167*, 729–736. [[CrossRef](#)]
25. Gibson, L.J. The hierarchical structure and mechanics of plant materials. *J. R. Soc. Interface* **2012**, *9*, 2749–2766. [[CrossRef](#)]
26. Barthelat, F.; Zhen, Y.; Buehler, M.J. Structure and mechanics of interfaces in biological materials. *Nat. Rev. Mater.* **2016**, *1*, 16007. [[CrossRef](#)]

27. Grishkewich, N.; Mohammed, N.; Tang, J.; Tam, K.C. Recent advances in the application of cellulose nanocrystals. *Curr. Opin. Colloid* **2017**, *29*, 32–45. [[CrossRef](#)]
28. Xing, D.; Li, J.; Wang, X.; Wang, S.Q. In situ measurement of heat-treated wood cell wall at elevated temperature by nanoindentation. *Ind. Crop. Prod.* **2016**, *87*, 142–149. [[CrossRef](#)]
29. Ben, D.B.; James, F.S. High-temperature nanoindentation testing of fused silica and other materials. *Philos. Mag. A* **2002**, *82*, 2179–2186.
30. Stanzl-Tschegg, S.; Beikircher, W.; Loidl, D. Comparison of mechanical properties of thermally modified wood at growth ring and cell wall level by means of instrumented indentation tests. *Holzforschung* **2009**, *63*, 443–448. [[CrossRef](#)]
31. Marcio, R.S.; José, O.B.; José, S.G.; Gilmará, O.M.; Carlito, C.J.; André, L.C.; Francisco, A.R.L. Chemical and Mechanical Properties Changes in Corymbia Citriodora Wood Submitted to Heat Treatment. *Int. J. Mater. Eng.* **2015**, *5*, 98–104.
32. Zickler, G.A.; Schöberl, T.; Paris, O. Mechanical properties of pyrolysed wood: A nanoindentation study. *Philos. Mag.* **2006**, *86*, 1373–1386. [[CrossRef](#)]
33. Xu, F.; Long, Z.L.; Deng, X.H.; Zhang, P. Loading rate sensitivity of nanoindentation creep behavior in a Fe-based bulk metallic glass. *Trans. Nonferrous Met. Soc. China* **2013**, *23*, 1646–1651. [[CrossRef](#)]
34. Chen, Y.H.; Huang, J.C.; Wang, L.; Nieh, T.G. Effect of residual stresses on nanoindentation creep behavior of Zr-based bulk metallic glasses. *Intermetallics* **2013**, *41*, 58–62. [[CrossRef](#)]
35. Mukudai, J.; Yata, S. Modeling and simulation of viscoelastic behavior (tensile strain) of wood under moisture change. *Wood Sci. Technol.* **1986**, *20*, 335–348. [[CrossRef](#)]